Biophysical Chemistry 205 (2015) 24–32

Contents lists available at ScienceDirect

Biophysical Chemistry

journal homepage: http://www.elsevier.com/locate/biophyschem

PIP2 and PIP3 interact with N-terminus region of TRPM4 channel

Kristyna Bousova [a,b], Michaela Jirku [b,c], Ladislav Bumba [d], Lucie Bednarova [e], Miroslav Sulc [d], Miloslav Franek [f], Ladislav Vyklicky [b], Jiri Vondrasek [e], Jan Teisinger [b,*]

[a] 2nd Faculty of Medicine, Charles University in Prague, 15006 Prague, Czech Republic
[b] Institute of Physiology, Academy of Sciences of the Czech Republic, 14220 Prague, Czech Republic
[c] Faculty of Science, Charles University in Prague, 12843 Prague, Czech Republic
[d] Institute of Microbiology, Academy of Sciences of the Czech Republic, 14220 Prague, Czech Republic
[e] Institute of Organic Chemistry and Biochemistry, Academy of Sciences of the Czech Republic, 16610 Prague, Czech Republic
[f] 3rd Faculty of Medicine, Charles University in Prague, 10000 Prague, Czech Republic

HIGHLIGHTS

- TRPM4 N- terminus channel contains binding site for potential regulatory molecules PIP2 and PIP3
- Basic R755 and R767 amino acids of TRPM4 N-terminal were determined to interact with the PIP2/PIP3 molecules directly
- TRPM4 fusion protein segments do not change its secondary structure content during complex formation with PIP2 or PIP3
- Molecular model of TRPM4 segment with PIP2 docking confirmed non-covalent binding mode

GRAPHICAL ABSTRACT

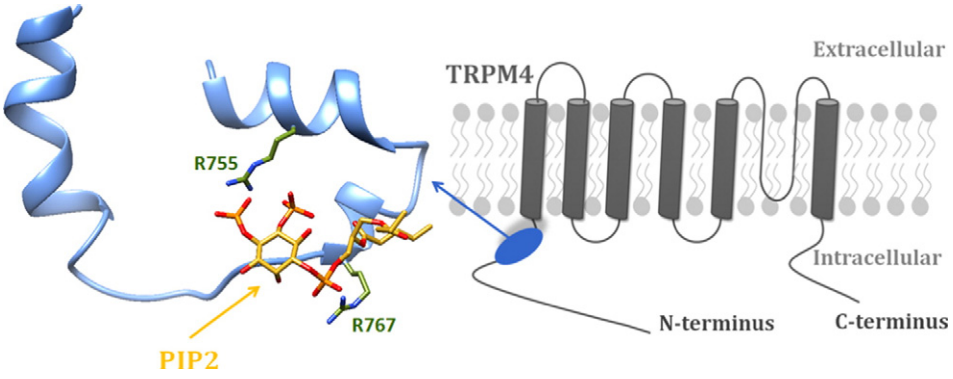

ARTICLE INFO

Article history:
Received 14 April 2015
Received in revised form 4 June 2015
Accepted 6 June 2015
Available online 9 June 2015

Keywords:
TRPM4 channel
PIP2
Binding site
Surface plasmon resonance
Molecular modeling
Circular dichroism

ABSTRACT

The transient receptor potential melastatin 4 (TRPM4) is a calcium-activated non-selective ion channel broadly expressed in a variety of tissues. Receptor has been identified as a crucial modulator of numerous calcium dependent mechanisms in the cell such as immune response, cardiac conduction, neurotransmission and insulin secretion. It is known that phosphoinositide lipids (PIPs) play a unique role in the regulation of TRP channel function. However the molecular mechanism of this process is still unknown. We characterized the binding site of PIP2 and its structural analogue PIP3 in the E733–W772 proximal region of the TRPM4 N-terminus via biophysical and molecular modeling methods. The specific positions R755 and R767 in this domain were identified as being important for interactions with PIP2/PIP3 ligands. Their mutations caused a partial loss of PIP2/PIP3 binding specificity. The interaction of PIP3 with TRPM4 channels has never been described before. These findings provide new insight into the ligand binding domains of the TRPM4 channel.

1. Introduction

Transient receptor potential channels (TRPs) are non-selective ion channels that play a unique role in cell sensor systems and are involved

* Corresponding author.
E-mail address: jan.teisinger@fgu.cas.cz (J. Teisinger).

http://dx.doi.org/10.1016/j.bpc.2015.06.004
0301-4622/

in many calcium-mediated cell functions [1,2]. TRPs are a diverse family of proteins expressed in many organisms, tissues and cell types. Their variety is demonstrated by proposed functions: transmission of painful stimuli, modulation of vascular tone, involvement in pathogenesis of diabetes mellitus, supply of intracellular calcium stores and modulation of cell cycle, [3,4]. In sensory neurons, TRPs contribute to many of activities including thermal sensation, homeostasis of body temperature and pain [5]. In the central nervous system (CNS), they have been associated with synaptic transmission, neurogenesis and brain development [6,7]. These special nociceptive receptors are transporters of mono and bivalent cations into the cell [3]. The structure of TRPs was unknown for a long time, despite numerous crystallization attempts to resolve their structure, recently almost the entire three-dimensional structure of the vanilloid 1 (TRPV1) and ankyrin 1 (TRPA1) receptor was determined by single-particle electron cryo-microscopy [8–10]. All members of the TRP superfamily share the same membrane topology. They have six transmembrane helices (TM) with a pore region between TM5–TM6 (Fig. 1A) and all of them have a homotetrameric structure [11–14]. Intracellularly located N- and C-tails are responsible for the regulation of TRP channels, which carry binding sites for signal ligands such as the intracellular calcium binding protein calmodulin [15,16] or plasma membrane lipid phosphatidylinositol-4,5-bisphosphate (PIP2) [17–20].

There is significant sequence similarity between TRPV, TRP canonical (TRPC) and TRP melastatin (TRPM), but no conservation between the N-terminal region of TRPM and those of TRPV and TRPC has been noted. On the other hand, the C-terminal domains of those three channels exhibit very high conservation in the proximal region (so-called TRP box) [21–24]. The TRPM family consists of eight members, which can be subdivided into four groups based on their sequence homology: M1 and M3, M4 and M5, M6 and M7, M2 and M8 [25]. TRPM4 is a calcium-activated non-selective ion channel that mediates the transport of monovalent cations (Fig. 1A). The activity of the encoded protein increases with increasing intracellular calcium concentration, but this channel does not transport calcium [26–28]. TRPM4 participates in ongoing processes in neurons [29,30], cardiomyocytes [31], pancreas cells [32], T-cells [33,34] and a link has been proven between defects in the TRPM4 receptor and progressive familial heart block type 1B [31].

Nowadays, more than 50 endogenous lipids and lipid-like molecules have been identified as direct activators or inhibitors of TRP channels. Regulators form lipids from a variety of metabolic pathways, including metabolites of the cyclooxygenase, lipooxygenase and cytochrome P450 pathways, phospholipids and lysophospholipids [35]. The most studied modulators of TRP channel function are phosphoinositides [18,38–40], which appear as the major regulators of this family ion channels. PIP2 and its structural analogue phosphatidylinositol-3,4,5-trisphosphate (PIP3) belong to the group of phosphoinositides that are low-abundant members of plasma membrane. These phospholipids function in a number of crucial cellular processes, such as plasma membrane-cytoskeleton linkages, second messenger signaling, regulation of proteins involved in phospholipid metabolism, cell adhesion and motility, and membrane trafficking [36,37]. PIP2 binding and regulation in TRPM receptors have also been studied extensively. It has been found that PIP2 activates TRPM3 [19], TRPM4 [41], TRPM5 [42], TRPM7 [43,44] and TRPM8 [45] channels. Analysis of the primary structure of the TRPM4 N-terminus revealed that PIP2 binding motif is conserved [46]. Under physiological conditions the phosphatidylinositols (PIPs) are negatively charged, the interactions of PIPs with the intracellular regions of ion channels, including TRPs, involve regions characterized by the presence of several positively charged residues [47–49]. Mutation of these positive residues has a critical role on PIP2 binding and this can lead to a PIP2-mediated channel regulation [39,50,51]. In some cases, binding is mediated by dedicated lipid-binding domains, one of the most known is the Pleckstrin Homology (PH) domain [52]. The elucidation of the crystal structure of K^+ channels with bound PIP2 provided the first atomistic description of a molecular mechanism by which PIP2 regulates channel activity and how it induces large conformation changes in the protein [53,54]. Whether or not the PIP2 modulation of TRPs involves similar conformational changes is still unknown. Moreover, some specific positively charged regions (e.g. PH domains) in TRPs could mediate the interaction with other PIPs with higher binding affinity — e.g. PIP3 [49,55,56].

In this study we addressed the localization of putative PIP2 and PIP3 binding site in the cytoplasmic domain of TRPM4 N-terminus using a combination of biophysical and molecular modeling tools. The proximal region E733–W772 of the N-terminus directly interacts with PIP2 and PIP3. According to the data presented, the binding affinity of PIP2 and PIP3 to studied N-terminus region of TRPM4 is approximately the same. The key residues R755 and R767 have been determined to be involved in PIP2/PIP3 binding. These findings provide new insight into the ligand binding domains of the TRPM4 channel.

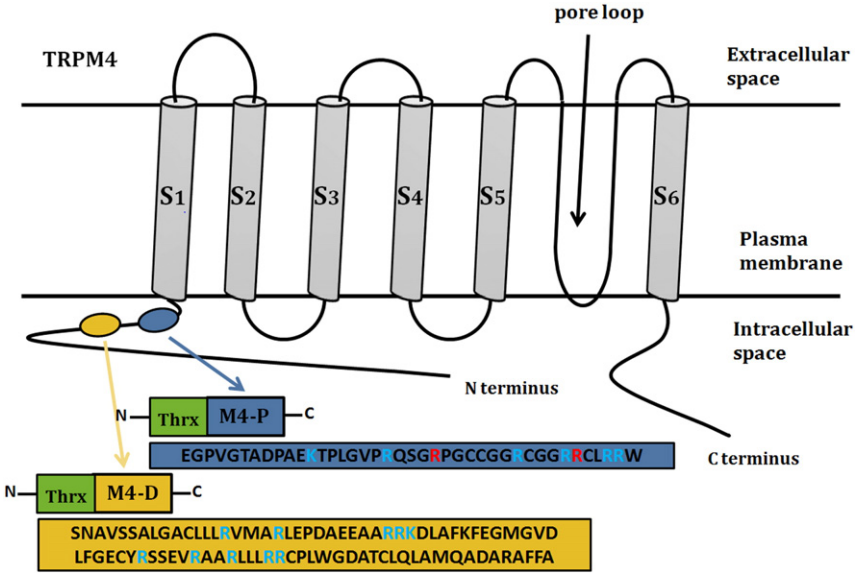

Fig. 1. Architecture of TRPM4 channel. The violet and yellow colored ovals show the location of the putative PIP2/PIP3 binding sites on N-terminus of TRPM4. The frames displayed proposed fusion (thioredoxin in green) protein constructs M4-D and M4-P. Their sequences displayed bellow show putative PH binding domains (blue letters). M4-P sequence shows amino acids involved in the interaction with PIP2 and PIP3 (red letters).

2. Materials and methods

2.1. Cloning of expression vectors and site-directed mutagenesis

cDNA constructs coding the appropriate human TRPM4 (UniProtKB/Swiss-Prot: Q8TD43.1) N-termini distal (residues S583–A669, henceforth denoted as M4-D) and proximal (residues E733–W772, henceforth denoted as M4-P) regions. These were subcloned into the BamHI and NotI sites of the pET32b expression vector (Novagen). Mutagenesis was performed using Pfu Ultra High-fidelity DNA polymerase (Stratagene) according to the manufacturer's instructions. Selected positive amino acid residues were replaced with Ala. All clones were verified by DNA sequencing.

2.2. Fusion expression and purification of TRPM4 N-termini constructs

M4-D and M4-P constructs and double mutant were expressed fused with thioredoxin and 2× His-tag on the N- and C- termini in Rosetta cells. Bacteria were transformed with the indicated construct. Overnight starter cultures (5 ml) were used to inoculate cultures, these were grown at 37 °C until they reached $OD_{600} = 0.6$ Isopropyl-1-thio-β-D-galactopyranoside (0.5 mM) was then added and induction proceeded for 20 h at 25 °C. After pelleting the bacteria, cells were resuspended in solutions containing the following: 10 mM PBS, 1 M NaCl, 10 mM imidazole, 0,05% NP-40, 0.1 mM PMSF and 1 mM β-mercaptoethanol, (pH 7.7 for M4-D and pH 8.2 for M4-P). Large scale bacterial cultures were lysed with a sonicator (Misonix Sonicator 300, USA). Lysates were spun at 40,000 rpm for 40 min at 4 °C. The fusion proteins were purified in two step chromatography techniques. At first, affinity chromatography was used in a chelating Sepharose fast flow column (Amersham Biosciences). The fusion proteins were eluted with the following: 10 mM PBS, 500 mM NaCl, 2 mM β-Mercaptoethanol, and 400 mM imidazol, (pH 7.7 for M4-D and pH 8.2 for M4-P). Gel permeation chromatography in a Superdex 75 column (Amersham Biosciences) was used as a second purification step. The proteins were eluted with 25 mM HEPES, 250 mM NaCl, 2 mM β-MerkaptoEtOH, 0.1% Tween and 10% glycerol, (pH 7.7 for M4-D and pH 8.2 for M4-P). Protein samples were concentrated using spin columns for protein concentration (Millipore). The purity was verified using 15% SDS-polyacrylamide gel electrophoresis (PAGE).

2.3. Mass spectrometry

The integrity of purified fusion proteins was checked by MALDI-TOF, mass spectra were acquired using an UltraFLEX III mass spectrometer (Bruker-Daltonics, Bremen, Germany). Protein bands from M4-D and M4-P, were digested with trypsin endoprotease (Promega) directly in the gel after destaining and cysteine modification by iodoacetamide [57]. The resulting peptide mixtures were extracted and loaded onto the MALDI-TOF/TOF target with α-cyano-4-hydroxycinnamic acid as the matrix. Peptide identities were verified using MS/MS fragmentation of the molecules, determination of the molecular mass of the fragments, and comparison with predicted (UniProtKB/Swiss-Prot: Q8TD43.1) and experimentally obtained fragmentation patterns.

2.4. Liposome preparation

The lipids L-a-phosphatidylinositol-4,5-bisphosphate (PIP2), 1,2-dioleoyl-*sn*-glycero-3-phospho-(1′-myo-inositol-3′,4′,5′-trisphosphate) (PIP3) and 1,2-dimyristoyl-sn-glycero-3-phosphocholine (PC) were obtained from Avanti Polar Lipids, Inc. A stock solution of PIP2 and PIP3 was prepared in a chloroform: methanol: H_2O (20:9:1) mixture, a stock solution of PC only in chloroform. Liposomes of the following compositions were prepared: PC, PC/PIP2 50/50% and PC/PIP3 50/50% by mixing appropriate volumes of the stock solutions. After being dried under an N2 stream, lipid films were hydrated with Hanks' Balanced Salt Solution (HBSS) buffer (25 mM HEPES, 250 mM NaCl) followed by extrusion 21 times through a polycarbonate membrane with Nuclepore Track-Etched Membranes with 100 nm pore diameter (Avanti Lipids, USA). The liposomes obtained were then centrifuged (50,000 *g*) for 30 min at 4 °C. The vesicles were diluted to a final concentration of 100 μg/ml in HBSS.

2.5. Surface plasmon resonance

SPR measurements were performed at 25 °C using a liposome-coated NLC sensor chip (Bio-Rad, USA) mounted on a ProteOn XPR36 Protein Interaction Array System (Bio-Rad, USA). The liposomes were prepared as above besides that the hydrated lipids were incubated with 8 mM oligonucleotide 5′-TATTTCTGATGTCCACCCCC-3′, modified at the 3′ end with cholesterol (Generi Biotech, Czech Republic). The mixture was extruded through a 100-nm polycarbonate membrane (Avanti Lipids, USA) and the freshly-formed liposomes were incubated with 8 mM anti-sense oligonucleotide 5′-TGGACATCAGAAATACCCCC-3′, modified at the 3′ end with biotin (Generi-Biotech, Czech Republic). After 15 min of incubation, the non-bound biotinylated oligonucleotide was removed by centrifugation (50,000 *g* for 30 min at 4 °C). The pelleted vesicles were resuspended to a final concentration of 100 μg/ml in HBSS buffer and immediately immobilized on the streptavidin-coated NLC chip surface. All SPR experiments were carried out in HBSS buffer at a flow rate of 30 μl/min for both association and dissociation phases of the sensograms. The proteins were serially diluted in the running buffer and injected in parallel ("one-shot kinetics") over the immobilized liposome surfaces. Surfaces were typically regenerated with 100 μl of 50 mM NaOH and 150 mM NaCl. The sensograms were corrected for sensor background by interspot referencing (the sites within the 6 × 6 array which are not exposed to ligand immobilization but are exposed to analyte flow), and double referenced by subtraction of analyte (channels 1–5) using a "blank" injection (channel 6). The data were analyzed by using a ProteOn software (Bio-Rad, USA) and fitted with a 1:1 Langmuir-type and heterogeneous binding models to determine association (ka) and dissociation (kd) rate constants. The Langmuir-type model assumes the interaction between liposomes (L) and protein (P) resulting in a direct formation of the final complex (LP)

$$L + P \underset{kd}{\overset{ka}{\rightleftharpoons}} LP$$

where ka and kd are the association and the dissociation rate constants, respectively. The heterogeneous binding models assumes two binding sites on the ligand

$$L1 + P \underset{kd1}{\overset{ka1}{\rightleftharpoons}} L1P; \quad L2 + P \underset{kd1}{\overset{ka2}{\rightleftharpoons}} L2P$$

where L1 and L2 are two separate binding sites on the ligand and P is the analyte protein. Note that there are two separate sets of association and dissociation rate constants (ka1/kd1 and ka2/kd2) to describe each binding event. The binding response of a sensorgram from a heterogeneous ligand then, is the sum of the binding response of two separate binding events. An apparent equilibrium dissociation constant, KD was determined as KD = kd/ka.

2.6. Circular dichroism measurements

The electronic circular diochroism (ECD) spectra of M4-D and M4-P were collected with a Jasco J-815 CD spectrometer (Jasco Corporation, Tokyo, Japan) in spectral range 200–300 nm using 0.1 cm path length quartz cell at room temperature. The experimental setup was as follows: 0.5 nm step resolution, 10 nm/min speed, 16 s response time and 1 nm bandwidth. The sample concentration was kept constant 0.1 mg/ml in 25 mM HEPES (pH = 8.0) and 250 mM NaCl. The proteins were measured also with trifluorethanol (TFE) mixture (50% v/v TFE)

and in the presence of liposomes (final liposome concentration was 5 μM). After baseline correction, the final spectra were expressed as a molar ellipticity θ (deg·cm^2·dmol^{-1}) per residue. Secondary structure content was determined using an online circular dichroism analysis program Dichroweb software [58].

2.7. Molecular modeling

The 3D model of fusion construct — human TRPM4 N-terminus (UniProtKB/Swiss-Prot: Q8TD43.1; positions E733–W772, M4-P) with thioredoxin was generated by the I-Tasser prediction server [59,60]. The final model for construct was carefully selected, satisfying the criteria of Arg residue exposure to the solvent and geometry constraints of the potential ligand binding site. Docking PIP2 (ligand in 3SPI) and PIP3 (ligand in 1W1G) ligands were performed in Molecular Operating Environment (MOE) with the Induced Fit protocol [61]. The optimal binding mode was selected by applying the lowest interaction energy and best geometry fit criteria. Two molecular representations were generated using Chimera [62].

3. Results

3.1. Design and purification of TRPM4 constructs

We localized arginine and lysine rich regions to search for potential PIP2/PIP3 binding motif present in the intracellular termini of human TRPM4. Two putative PIP2/PIP3 binding sites M4-D and M4-P (regions 583–669 and 733–772) were predicted (Fig. 1). We cloned cDNA of these regions into a pET32_b vector for protein expression in Rosetta cells. To improve the solubility and expression yield of the proteins (wild type and its site directed mutants), we expressed and purified all of them as fusion proteins with the thioredoxin-tag at the N-terminus and 6× His tag at both N-termini. All expressed fusion proteins were soluble and in sufficient amounts to perform the binding experiments.

3.2. Analysis of PIP2/PIP3 binding to M4-D and M4-P peptides by surface plasmon resonance

To gain insight into the interactions of M4-D and M4-P with PIP2 and PIP3, we utilized surface plasmon resonance (SPR) technology. PIP2 or PIP3 was incorporated into liposomes by extrusion of the hydrated lipid mixtures (PC, PC/PIP2 and PC/PIP3) through membranes with a 100-nm pore size and the freshly-prepared lipid vesicles were immobilized to a neutravidin-coated NLC sensor chip through a biotin/cholesterol-functionalized DNA linker. The DNA linker consists of a short DNA sequence that is bi-functionalized with cholesterol and biotin, which the former is embedded within the lipid bilayer of liposomes, while the latter associates with neutravidin on the sensor chip to couple the lipid vesicles to the sensor surface. To minimize mass transfer effect, several coupling concentrations of liposomes leading to refractive index changes of 500, 1000, and 1500 RU were tested. Initial experiments at each of these liposome-coating concentrations were conducted with the TRPM4 fusion proteins at concentrations ranging from 0 to 10 μM. Initial estimates of koff values showed concentration dependence at coupling levels of 1000 and 1500 RU indicating mass transfer effects. However, coupling level of 500 RU resulted in clear responses and concentration independence of koff at flow rates of 30 μl/ml (data not shown). Consequently, coupling level of about 500 RU and flow rate of 30 μl/ml were used for the remaining experiments.

Real time interaction of serially-diluted M4-D and M4-P proteins with lipid surfaces revealed typical concentration-dependent binding curves (Figs. 2 and 3). Binding of the thioredoxin fusions was exclusively mediated through the TRPM4 segments, since thioredoxin itself did not bind the lipid surface (Fig. 2A–C). Kinetic parameters of the interaction between M4-D and PC, PIP2 and PIP3 enriched vesicles were calculated from global fitting of concentration-dependent binding curves (Fig. 2D–F). The experimental binding curves for M4-D fitted well to a simple 1:1 Langmuir binding model, revealing that the interaction of M4-D with lipid membrane follows pseudo first order kinetics and the adsorption of M4-D on lipid surfaces is limited by a finite number of identical binding sites. Moreover, the interaction of M4-D with lipids appears to be transient, suggesting that the M4-D segment of the TRPM4 channel does not embed in the lipid bilayer. However, kinetic rate constants were of similar values regardless of the presence or absence of PIP2 or PIP3, indicating no specificity of the M4-D segment of TRPM4 for polar heads of PIP2 and PIP3 lipids protruding out of the lipid membranes (Table 1).

Fig. 3A shows the experimental binding curves for the interaction of M4-P with liposomes made from phosphatidylcholine (PC) alone. The extensive fitting of the binding curves showed that these data could not be fitted to either 1:1 Langmuir binding model or other binding models, such as, heterogeneous analyte, heterogeneous ligand, and conformation change models. Moreover, the intensities of the response (RU) at the end of the association phases (120 s) were found to be

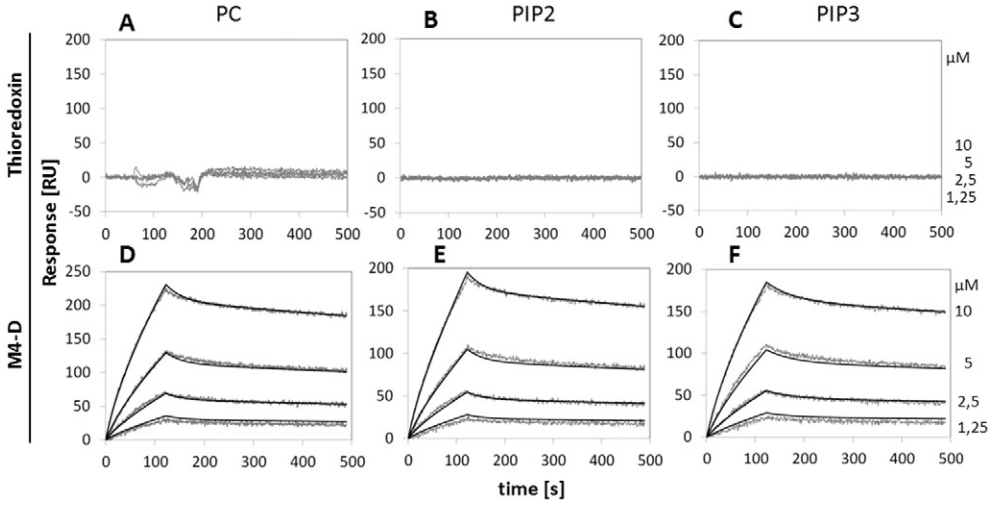

Fig. 2. SPR kinetic binding analysis of the interaction between M4-D and lipid vesicles. One-shot kinetic analysis of thioredoxin (A–C) and M4-D (D–F) interaction with liposomes containing phosphatidylcholine (PC) alone (A,D) or liposomes enriched with PIP2 (B,E) and PIP3 (C,F). Serially diluted proteins were injected in parallel over the sensor chip coated with 100-nm lipid vesicles and left to associate (120 s) and dissociate at constant flow rate of 30 μl/min. The kinetic data were globally fitted by using a heterogeneous ligand model (see Section 2). The fitted curves are superimposed as black lines on top of the sensograms.

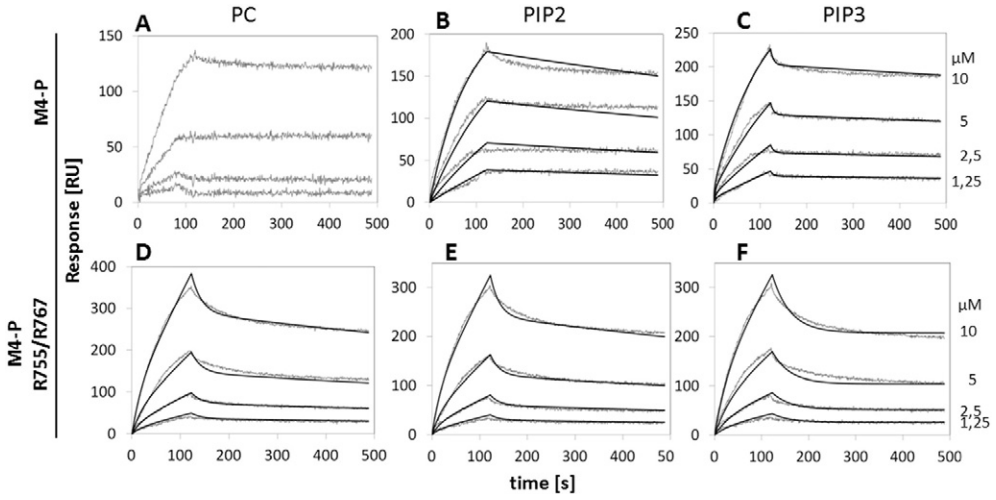

Fig. 3. SPR kinetic binding analysis of the interaction between M4-P and lipid vesicles. One-shot kinetic analysis of the interaction of M4-P (A–C) and its double mutant M4-P — R755A/R767A (D–F) with PC (A,D), PIP2 (B,E) and PIP3 enriched (C,F) lipid vesicles. Serially diluted proteins were injected in parallel over the sensor chip coated with 100-nm lipid vesicles and left to associate (120 s) and dissociate at constant flow rate of 30 μl/min. Apart from the interaction of M4-P with PC (A), which could not be fitted to any of the binding models, the kinetic data were globally fitted by using a heterogeneous ligand model (see Section 2). The fitted curves are superimposed as black lines on top of the sensograms.

linearly dependent on the concentration of the injected protein, indicating a non-specific interaction of M4-P with the lipid surface. In line with this observation, the data for the interaction of M4-P with PIP2 and PIP3 could not be fitted to a simple 1:1 binding model. Linear transformation of the association phase of the binding curves revealed nonlinear plots, demonstrating a more complex kinetics of the interactions. We then attempted to fit the binding curves to complex models to investigate the nature of these interactions. The data showed a close fit to a heterogeneous ligand model (Fig. 3B-C). The heterogeneous ligand model assumes that analyte (M4-P) binds two separate binding sites on the ligand (liposomes) and each ligand site binds the analyte independently with a different set of rate constants. The calculated association and dissociation rate constants (ka1, ka2, kd1, and kd2) as well as KD1 and KD2 for the interaction are listed in Table 2. The data analysis revealed that the affinities of M4-P to PIP2 and PIP3-enriched vesicles were comparable and found to be KD1 = 0.31 μM and KD2 = 5.5 μM for PIP2, and KD1 = 0.54 μM and KD2 = 5.4 μM for PIP3, respectively. In view of the fact that the heterogeneous ligand model assumes M4-P binding at two distinct sites with the binding affinity being approximately ten times higher for the first than the second site and simultaneously M4-P interacts non-specifically with liposome membranes made from PC alone, one can speculate that low-affinity KD2 values of the model corresponds to the non-specific interaction of M4-P with the PIP2- or PIP3-enriched vesicles, while high-affinity KD1 values could be attributed to the specific interaction of M4-P with polar heads of PIP2 or PIP3 on the lipid surfaces. Thus, the heterogeneous ligand model is the most likely model of the interaction of M4-P with PIP2- and PIP3-enriched vesicles.

Specificity of M4-P to PIP2 and PIP3 was further analyzed on a double mutant carrying substitution of two highly conserved arginine residues (R775 and R767) within a putative consensus motif (R/K-X12-14-R/K-X-R) that usually mediates high affinity binding of the PH domain to PIP3. In agreement with the wild-type construct, the binding curves for the interaction of the M4-P-R755A/R767A mutant with lipid vesicles were fitted to the heterogeneous ligand model (Fig. 3D–F). The calculated association and dissociation rate constants are listed in Table 2. Overall comparison of KD values revealed significant decrease in the binding affinity for the mutant. The main reason that contributes to the decreased binding affinity of the mutant was the faster dissociation (ka1) and slower association rates (kd1) of the arising complex. Moreover, the kinetics of interaction of the double mutant did not reveal any significant differences between binding to PC and PIP2- and PIP3-enriched vesicles indicating a complete loss of specificity for binding to PIP2 or PIP3. Thus, the M4-P segment of TrpM4 appears to interact specifically with PIP2 or PIP3 on the membrane surface and arginine residues R755 and R767 play an important role in this process.

3.3. Analysis of the secondary structure of M4-D and M4-P by circular dichroism

The secondary structure of the M4-D and M4-P fusion proteins was studied by ECD spectroscopy. Whereas the structure of cytosolic regions of TRPM4 is still unknown, the secondary structural composition of M4-D and M4-P fusion proteins with thioredoxin was determined as to be mostly disordered (Fig. 4 Table 2). ECD spectra of M4-D and M4-P fusion proteins confirmed that proteins are mostly unstructured, which is in a good agreement with the theoretical prediction based on their primary structure. According ECD spectra, both proteins M4-D and M4-P in the presence of liposomes formed by PC alone or PC containing PIP2/PIP3 (50/50%) do not change their secondary structure content (Fig. 4A, B and Table 2). This suggests that binding PIP2 or PIP3 to M4-D and M4-P proteins has no significant influence on their structure. According to our results based on 3D modeling of M4-P construct (Fig. 5), the model showed higher alpha helix content. While TFE is known as helix promoting solvent we also measured ECD spectra of M4-D and M4-P in the presence of TFE (Fig. 4C, D and Table 3) to estimate their ability to form α-helical structure [63–65]. The ECD spectra revealed that in the presence of TFE both proteins adopt helical structure more easily. A fraction of particular secondary structures obtained by analysis of ECD data corresponds to theoretical predictions from molecular modeling. This suggests that M4-D and M4-P in TFE environment could probably adopt a structure similar to their predicted fold. (See Table 4.)

Table 1
Kinetic and binding affinity constants for the interactions of M4-D with PC, PIP2 and PIP3 enriched lipid vesicles.

		ka × 10^2 [$M^{-1}\cdot s^{-1}$][a]	kd × 10^{-4} [s^{-1}]	KD [μM][b]
M4-D	PC	4.3 ± 1.2	6.5 ± 2.1	1.5 ± 0.6
	PIP2	2.5 ± 0.8	6.6 ± 2.4	2.6 ± 0.8
	PIP3	4.0 ± 1.3	6.5 ± 1.9	1.6 ± 0.7

[a] Results are means ± S.D. from the analysis of two independent measurements.
[b] The equilibrium dissociation constant (KD) was determined as ka/kd.

Table 2
Kinetic and binding affinity constants for the interactions of M4-P proteins with PC, PIP2 and PIP3 enriched lipid vesicles.

		ka1 × 10^3 [$M^{-1}\cdot s^{-1}$][a]	kd1 × 10^{-4} [s^{-1}]	KD1 [μM][b]	ka1 × 10^4 [$M^{-1}\cdot s^{-1}$]	kd2 × 10^{-1} [s^{-1}]	KD2 [μM]
M4-P	PC	–	–	–	–	–	–
	PIP2	1.5 ± 0.4	4.6 ± 1.1	0.3 ± 0.1	3.8 ± 0.8	2.1 ± 0.5	5.5 ± 1.4
	PIP3	1.2 ± 0.3	6.5 ± 2.1	0.5 ± 0.2	3.3 ± 0.7	1.8 ± 0.4	5.4 ± 1.3
R755/R767	PC	0.3 ± 0.1	9.8 ± 2.5	3.3 ± 0.9	4.1 ± 1.2	0.6 ± 0.2	1.5 ± 0.4
	PIP2	0.2 ± 0.1	10.1 ± 3.1	5.1 ± 1.4	5.2 ± 1.7	0.7 ± 0.2	1.3 ± 0.3
	PIP3	0.2 ± 0.1	9.9 ± 2.9	4.9 ± 1.5	3.2 ± 0.9	0.6 ± 0.2	1.9 ± 0.3

[a] Results are means ± S.D. from the analysis of two independent measurements.
[b] The equilibrium dissociation constants (KD1 and KD2) was determined as kd1/ka1 and kd1/ka1, respectively.

3.4. 3D modeling and PIP2/PIP3 docking of M4-P

To predict the interactions of the phospholipid binding site of TRPM4 N-termini with PIP2/PIP3 ligands, we created a 3D model of the corresponding M4-P N-terminus in fusion construct with thioredoxin (thioredoxin, 2× His-tags and TRPM4E733-W772 sequence). A model of human TRPM4 fusion protein was generated using the I-Tasser prediction server. The thioredoxin structure was deleted from the model and potential PIP2/PIP3 binding site was assigned by MOE. Eventually, PIP2 and PIP3 ligands were docked into the assigned binding site (Fig. 5). To orient PIP2/PIP3 ligands properly, we utilized structural information from the literature — in particular the interaction of PIP2 with the proximal region of the intracellular tails of potassium ion channels [53,54,66] which is well characterized. For the models of TRPM4-PIP2/PIP3 complexes we assumed that the interaction is accomplished by an arginine/lysine cluster interacting with the phosphate groups of PIP2 (PIP3). Positively charged amino acids are frequent in the vicinity of the inner plasma membrane leaflet where binding sites for regulatory molecules such as phosphatidylinositol phosphates are expected to be abundant. Their mutation to alanine residues causes a replacement of their charged-side chains in the binding site, which makes it less favorable for interaction with PIP2 [67–69]. According to this hypothesis, our in silico predictions support that R755A and R767A mutations result in the loss of non-covalent interactions with the phosphate groups of PIP2/PIP3 which is in agreement with our experimental data.

4. Discussion

PIP2 and PIP3 are short-lived phospholipids found on the cytosolic side of eukaryotic cell membranes and act as regulators of signaling proteins in the plasma membrane that induce a TRP channels [46,67]. It has been shown that many ion receptors — inward-rectifier and voltage-gated K^+ channels, Ca^{2+} channels, cyclic nucleotide gated channels, epithelial Na^+ and Cl^- channels are regulated by PIP2 [70]. Of the many described phospholipid-binding proteins, a number of different domain structures have been defined that exhibit stereospecific recognition of specific phosphoinositide head groups in the context of cellular membrane surfaces these include the pleckstrin homology (PH) and Phox-homology (PX) domains. The common hypothesis to explain the binding of PIP2 is that positively charged residues present in the domain are responsible for the ligand-dependent modulation of the TRP's activity. Similarly, TRP channels also contain intracellular domain clusters which have been identified as PIP2 binding pockets [49,71]. The regulation of TRPs by phosphoinositides, especially by PIP2 and PIP3, has only been described for the TRPC subfamily [55]. It was found that PIP3 bound TRPC6 directly with the highest potency. Biophysical and bioinformatics methods were used to improve our

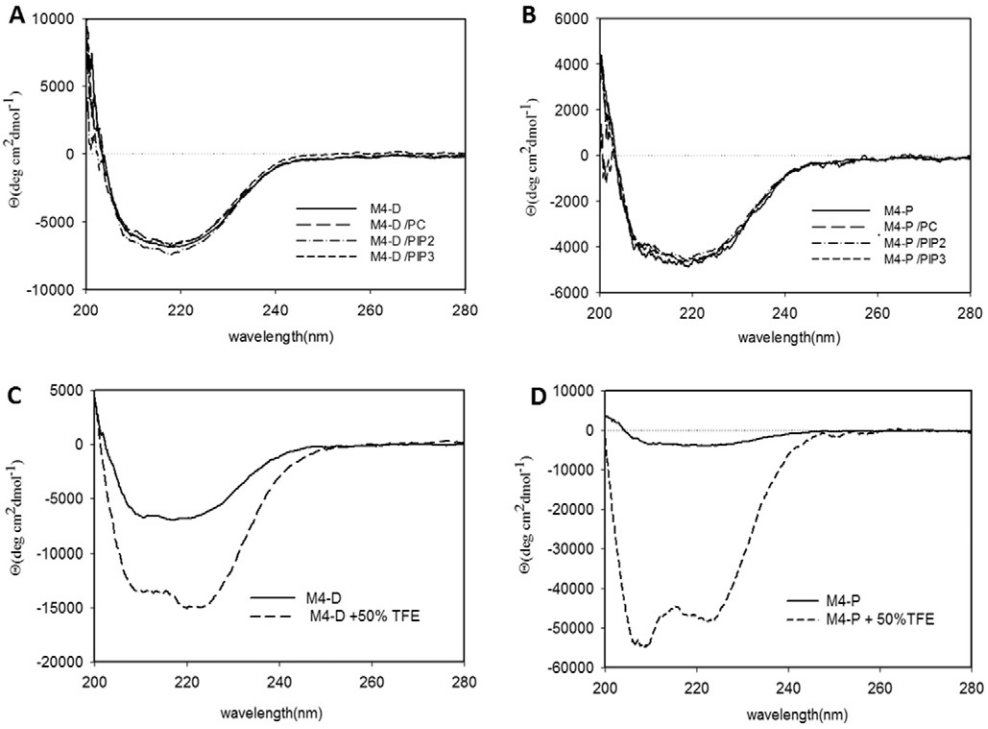

Fig. 4. ECD spectra of peptide M4-D and M4-P in presence of liposomes and TFE. Peptide M4-D (A) and M4-P (B) in the interaction with PC, PIP2 and PIP3 enriched lipid vesicles. Peptides M4-D (C) and M4-P (D) in the presence of 50% (v/v) TFE. CD spectra were expressed as molar ellipticity Q ($deg\cdot cm^2\cdot dmol^{-1}$) per residue.

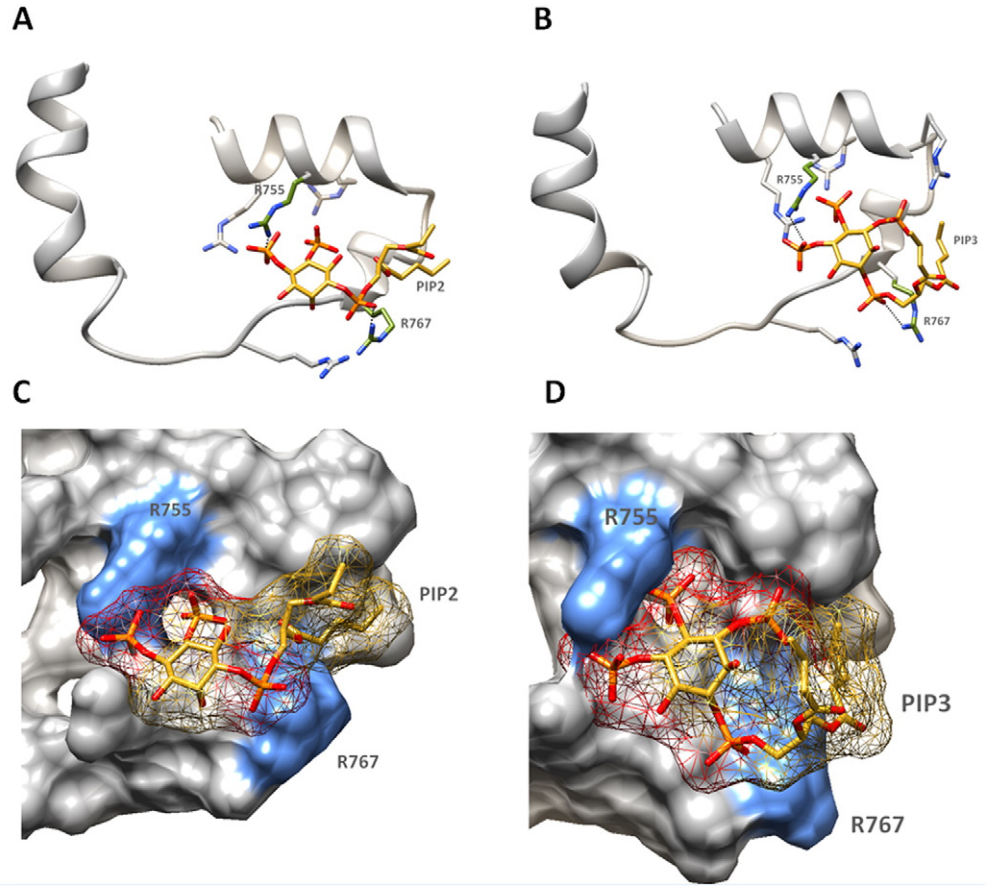

Fig. 5. M4-P domain binds PIP2 and PIP3. (A) Schematic view of the interactions of M4-P/PIP2 and (B) M4-P/PIP3. All arginines exhibit similar binding to the PIP2 and PIP3. Important arginine residues bonded (dashed lines) to PIP2/PIP3 are colored green (R755 and R767). We used the following color convention: gray — protein backbone of the M4-P, yellow — carbon atoms of PIP2, oxygen (O_2) — red, nitrogen (N) — blue, phosphorus (P) — orange. (C) Solvent accessible surface representation of the M4-P/PIP2 and (D) M4-P/PIP3 complexes; surfaces of lysine and arginine R755, R767 colored blue.

understanding of the regulation of the TRPM4 channel by two similar ligands (PIP2/PIP3) and identify the binding sites or actual potential gating sites on the N-termini.

The regulation of TRPM channels by PIP2 was demonstrated [72]. A binding site for PIP2, calmodulin and calcium-binding protein A1 protein (S100A1) was found in the TRPM3 N-terminus and these ligands can compete with each other [14]. As for TRPM5, PIP2 promotes the gating of this channel, which, after desensitization, was activated by lower concentrations of Ca^{2+} in the presence of PIP2 [42]. The hydrolysis of PIP2 by phospholipase C (PLC)-coupled hormones may constitute an important pathway for TRPM6 gating [37,40,73]. The importance of PIP2 has also been reported for TRPM7, in which PIP_2 hydrolysis by PLCs inhibits channel activation [43,44]. The breakdown of PIP2 also appears to underlie the desensitization of TRPM8 [45]. Because PIP2 is degraded by PLC, the action of PIP2 may underlie the response of some TRPs to the stimulation of PLC-coupled plasma membrane receptors, as mentioned above for TRPM7 [44]. In the intracellular C-terminus region of the TRPM4 channel, the PIP2 binding site in the TRP box domain was described by electrophysiology experiments. The group of Nilius et al. [41] investigated whether mutations in TRPM4-K1059, and R1062 in the TRP box domain affect the response to PIP2. It was demonstrated that PIP2 enhances the activity of TRPM4 Ca^{2+}-activated cation channels by decreasing Ca^{2+} sensitivity and shifting their voltage dependence, and provided evidence that these effects require an intact C-terminal PH domain. In contrast, the binding of PIP2 to the N-terminus of the TRPM4 channel has not been reported before.

Here we used surface plasmon resonance to directly study the specificity and binding affinity of TRPM4 constructs to liposomes containing PIP2/PIP3. We proposed the two putative binding sites M4-D and M4-P in close proximity to each other and rich in Arg/Lys residues, which can be important for interaction with PIP2 and PIP3. It was found out that M4-D could interact with lipid bilayer but without any specificity for PIP2 or PIP3 lipids, but M4-P fusion protein binds both ligands specifically. Dissociation constants for M4-P–PIP2/PIP3 complexes were very similar and were in the micro molar range. A similar binding affinity for PIP2 (PIP3) was observed previously with the TRP family members [19,20]. Two important residues in the N-termini PIP2/PIP3 binding domain were found, namely R755 and R767, their mutation caused complete loss of specificity for PIP2/PIP3 binding. Here it is shown that PIP3 binds the same region on the TRPM4 N-terminus with almost the same affinity as PIP2. Moreover, the mutations of positively charged

Table 3
Calculated incidence (%) of secondary structure content. M4-D and M4-P fusion protein constructs and their complexes with PIP2 and PIP3 determined by CD spectroscopy in 25 mM HEPES (pH = 8.0), 250 mM NaCl.

	Helix	Anti-parallel	Parallel	β-turn	Random coil
M4-D	22	11	11	17	38
M4-D/PC	22	11	11	17	39
M4-D/PIP2	21	11	11	17	38
M4-D/PIP3	22	11	12	17	38
M4-P	17	13	13	17	40
M4-P/PC	15	13	13	18	41
M4-P/PIP2	15	11	14	17	42
M4-P/PIP3	17	13	13	17	40

Table 4
Calculated incidence (%) of secondary structure content. M4-D and M4-P fusion protein constructs determined by CD spectroscopy in 25 mM HEPES (pH = 8.0), 250 mM NaCl and 1 mM $CaCl_2$, and in the same buffer with 50% TFE added.

	Helix	Anti-parallel	Parallel	β-turn	Random coil
M4-D	22	11	11	17	38
M4-D + TFE	44	6	7	15	27
M4-P	17	13	13	17	40
M4-P + TFE	95	0	0	4	1

residues within this domain affected the binding to PIP3, as was observed for PIP2.

Intracellular N- and C-termini are highly heterologous for every subfamily of the whole superfamily of TRPs. Circular dichroism measurements were used to obtain knowledge of the secondary structure of TRPM4 N-termini fusion proteins — individually, in complexes with ligands PIP2/PIP3 and in the TFE environment. The secondary structure of TRPM4 N-termini fusion proteins was determined to be mostly unstructured. In complexes of TRPM4-PIP2/PIP3 no changes were detected in the secondary structure of proteins. According to these data we can assume that TRPM4 proteins do not undergo structural changes upon complex formation. Moreover, both M4-D and M4-P fusion proteins readily adopt a helical structure in TFE buffer, it follows that these regions may acquire more structural characteristics in the in vivo environment.

Molecular model of the TRPM4 N-termini proximal regions interacting with PIP2/PIP3 suggests that the phosphate head groups of PIP2 and PIP3 form ionic interactions with positively charged arginines R755 and R767. PIP2 binding pocket is present in the M4-P region. According to the data from SPR, the binding affinity for M4-P–PIP2/PIP3 complexes is very similar. The molecular model with PIP3 supports our data from SPR, because the one extra phosphate group of PIP3 does not have a particularly large influence on the strength of the interaction. Using methods of molecular modeling, we localized a possible interaction mode of the PIP2 binding pocket in the proximal M4-P of TRPM4 domain with PIP2/PIP3, but the structural basis of the action by lipids on TRP channel activity has not been determined yet.

In conclusion, we have identified proximal region E733–W772 TRPM4 N-terminus as PIP2 binding pocket using SPR measurements. The basic amino acid R755 and R767 residues are crucial in the interaction with PIP2 and PIP3, their mutation caused a total loss of binding specificity to ligands. This is the first report to show that PIP3 binds directly to TRPM4 family channel. M4-P domain can bind both PIP2 and PIP3 with a similar binding affinity to share the same binding site. It can be assumed that the binding site for PIP2 is always shared for PIP3. It was confirmed, from the in silico docking experiments, that R755 and R767 residues interact with the phosphates of the PIP2/PIP3 molecules directly, according to the same mode as was previously published [53,54,67]. During the interaction of fusion proteins with LUVs enriched by PIP2/PIP3, M4-D and M4-P do not change their secondary structure content. Surely, phosphatidylinositol phosphates are important regulators in TRP channels and it is very likely that they could regulate TRPM4 channel via binding to its intracellular N-terminus in the same way as was reported for other members of the TRPM family [19,42–44,72,73], nevertheless more functional studies will be required to elucidate the role of PIP2 and PIP3 in TRPM4 channel gating and regulation.

Acknowledgments

This study was supported by the Grant Agency of Charles University (grant no. 842313, 238214), the Grant Agency of the Czech Republic (grant no. 207/11/0717 and 15-11851S), the Grant Agency of the Czech Republic Project of Excellence in the Field of Neuroscience (grant no. P304/12/G069) and with institutional support RVO: 67985823.

References

[1] F. Yi, H. Han, New insights into the TRP channel: interaction with pattern recognition receptors, Channels 8 (2014) 13–19.
[2] J. Vriens, K. Held, A. Janssens, B.I. Thót, S. Kerselaers, B. Nilius, R. Vennekens, T. Voets, Opening of an alternative ion permeation pathway in a nociceptor TRP channel, Nat. Chem. Biol. 10 (2014) 188–195.
[3] T. Smani, G. Shapovalov, R. Skryma, N. Prevarskaya, J.A. Rosado, Functional and physiological implications of TRP channels, Biochim. Biophys. Acta 1853 (2015) 1772–1782.
[4] A. Gordon-Shaag, W.N. Zagotta, S.E. Gordon, Mechanism of Ca^{2+}-dependent desensitization in TRP channels, Channels 2 (2008) 125–129.
[5] D. Julius, TRP channels and pain, Annu. Rev. Cell Dev. Biol. 29 (2013) 355–384.
[6] R. Vennekens, A. Menigoz, B. Nilius, TRPs in the brain, Rev. Physiol. Biochem. Pharmacol. 163 (2012) 27–64.
[7] M.B. Morelli, C. Amantini, S. Liberati, M. Santoni, M. Nabissi, TRP channels: new potential therapeutic approaches in CNS neuropathies, CNS Neurol. Disord. Drug Targets 12 (2013) 274–293.
[8] M. Liao, E. Cao, D. Julius, Y. Cheng, Structure of the TRPV1 ion channel determined by electron cryo-microscopy, Nature 504 (2013) 107–112.
[9] K.W. Huynh, M.R. Cohen, S. Chakrapani, H.A. Holdaway, P.L. Stewart, V.Y. Moissenkova-Bell, Structural insight into the assembly of TRPV1 channels, Structure 22 (2014) 260–268.
[10] C.E. Paulsen, J.P. Armache, Y. Gao, Y. Cheng, D. Julius, Structure of the TRPA1 ion channel suggests regulatory mechanisms, Nature 520 (2015) 511–517.
[11] D.E. Clapham, TRP channels as cellular sensors, Nature 426 (2003) 517–524.
[12] C.L. Huang, The transient receptor potential superfamily of ion channels, J. Am. Soc. Nephrol. 15 (2004) 1690–1699.
[13] M.M. Moran, H. Xu, D.E. Clapham, TRP ion channles in nervous system, Curr. Opin. Neurobiol. 14 (2004) 362–369.
[14] R. Padinjat, S. Andrews, TRP channels at a glance, J. Cell Sci. 117 (2004) 5707–5709.
[15] L. Grycova, Z. Lansky, E. Friedlova, V. Obsilova, T. Obsil, J. Teisinger, Ionic interactions are essential for TRPV1 C-terminus binding to calmodulin, Biochem. Biophys. Res. Commun. 375 (2008) 680–683.
[16] B. Holakovska, L. Grycova, M. Jirku, M. Sulc, L. Bumba, J. Teisinger, Calmodulin and S100A1 interact with N terminus of TRPM3 channel, J. Biol. Chem. 287 (2012) 16645–16655.
[17] T. Voets, B. Nilius, Modulation TRPs by PIPs, J. Physiol. 582 (2007) 939–944.
[18] B. Nilius, G. Owsianik, T. Voets, Transient receptor potential channels meet phosphoinositides, EMBO J. 27 (2008) 2809–2816.
[19] B. Holendova, L. Grycova, M. Jirku, J. Teisinger, PtdIns(4,5)P2 interacts with CaM binding domains on TRPM3 N-terminus, Channels 6 (2012) 479–482.
[20] L. Grycova, B. Holendova, L. Bumba, J. Bily, M. Jirku, Z. Lansky, J. Teisinger, Integrative binding sites within intracellular termini of TRPV1 receptor, PLoS ONE 7 (2012) e48437.
[21] T. Voets, B. Nilius, TRPs make sense, J. Membr. Biol. 192 (2003) 1–8.
[22] X. Jin, J. Touhey, R. Gaudet, Structure of the N-terminal ankyrin repeat domain of the TRPV2 ion channel, J. Biol. Chem. 281 (2006) 25006–25010.
[23] P.V. Lishko, E. Procko, X. Jin, C.B. Phelps, R. Gaudet, The ankyrin repeats of TRPV1 bind multiple ligands and modulate channel sensitivity, Neuron 54 (2007) 905–918.
[24] C.B. Phelps, R.J. Huang, P.V. Lishko, R.R. Wang, R. Gaudet, Structural analyses of the ankyrin repeat domain of TRPV6 and related TRPV ion channels, Biochemistry 47 (2008) 2476–2484.
[25] C. Harteneck, Function and pharmacology of TRPM cation channels, Naunyn Schmiedeberg's Arch. Pharmacol. 371 (2005) 307–314.
[26] P. Launay, A. Fleig, A.L. Perraud, A.M. Scharenberg, R. Penner, J.P. Kinet, TRPM4 is a Ca^{2+} activated nonselective cation channel mediating cell membrane depolarization, Cell 109 (2002) 397–407.
[27] M. Murakami, F. Xu, I. Miyoshi, E. Sato, K. Ono, T. Iijima, Identification and characterization of the murine TRPM4, Biochem. Biophys. Res. Commun. 307 (2003) 522–528.
[28] J.C. Yoo, O.V. Yarishkin, E.M. Hwang, E. Kim, D.G. Kim, N. Park, S.G. Hong, J.Y. Park, Cloning and characterization of rat transient receptor potential-melastatin 4 (TRPM4), Biochem. Biophys. Res. Commun. 391 (2010) 806–811.
[29] B. Schattling, K. Steinbach, E. Thies, M. Kruse, A. Menigoz, F. Ufer, V. Flockerzi, W. Bruck, O. Pongs, R. Vennekens, M. Kneussel, M. Freichel, D. Merkler, M.A. Friese, TRPM4 cation channel mediates axonal and neuronal degeneration in experimental autoimmune encephalomyelitis and multiple sclerosis, Nat. Med. 18 (2012) 1805–1811.
[30] Y.S. Kim, E. Kang, Y. Makino, S. Park, J.H. Shin, H. Song, P. Launay, D.J. Linden, Characterizing the conductance underlying depolarization-induced slow current in cerebellar Purkinje cells, J. Neurophysiol. 109 (2013) 1174–1181.
[31] M. Krause, E. Schulze-Bahr, V. Corfield, A. Beckmann, B. Stallmeyer, G. Kurtbay, I. Ohmert, E. Shultze-Bahr, P. Brink, O. Pongs, Impaired endocytosis of the ion channel TRPM4 is associated with human progressive familial heart block type I, J. Clin. Invest. 119 (2009) 2737–2744.
[32] H. Cheng, A. Beck, P. Launay, S.A. Gross, A.J. Stokes, J.P. Kinet, A. Fleig, R. Penner, TRPM4 controls insulin secretion in pancreatic beta-cells, Cell Calcium 41 (2007) 51–61.
[33] G. Barbet, M. Demion, I.C. Moura, N. Serafini, T. Léger, F. Vrtovsnik, R.C. Monteiro, R. Guinamard, J.P. Kinet, P. Launay, The calcium activated nonselective cation channel TRPM4 is essential for the migration but not the maturation of dendritic cells, Nat. Immunol. 9 (2008) 1148–1156.
[34] T. Shimizu, G. Owsianik, M. Freichel, V. Flockerzi, B. Nilius, R. Vennekens, TRPM4 regulates migration of mast cells in mice, Cell Calcium 45 (2009) 226–232.
[35] F.J. Taberner, G. Fernandéz-Ballester, A. Fernandéz-Carvajal, A. Ferrer-Montiel, TRP channels interaction with lipids and its implications in disease, Biochim. Biophys. Acta Biomembr. S0005–2736 (2015) 00101–00107.

[36] B. Hille, E.J. Dickson, M. Kruse, O. Vivas, B.C. Sush, Phosphoinositides regulate ion channels, Biochim. Biophys. Acta Mol. Cell Biol. Lipids 1851 (2014) 844–856.
[37] T. Rohacs, Phosphoinositide regulation of TRP Channels, Handb. Exp. Pharmacol. 223 (2014) 1143–1176.
[38] P. Raghu, R.C. Hardie, Regulation of *Drosophila* TRPC channels by lipid messengers, Cell Calcium 45 (2009) 566–573.
[39] E.D. Prescott, D. Julius, A modular PIP2 binding site as a determinant of capsaicin receptor sensitivity, Science 300 (2003) 1284–1288.
[40] T. Rohacs, Phosphoinositide regulation of non-canonical transient receptor potential channels, Cell Calcium 45 (2009) 554–565.
[41] B. Nilius, F. Mahieu, J. Prenen, A. Janssens, G. Owsianik, R. Vennekens, T. Voets, The Ca^{2+}-activated cation channel TRPM4 is regulated by phosphatidylinositol 4,5-biphosphate, EMBO J. 25 (2006) 467–478.
[42] D. Liu, E.R. Liman, Intracellular Ca^{2+} and the phospholipid PIP2 regulate the taste transduction ion channel TRPM5, Proc. Natl. Acad. Sci. U. S. A. 100 (2003) 15160–15165.
[43] T. Rohacs, B. Nilius, Regulation of transient receptor potential (TRP) channels by phosphoinositides, Pflugers Arch. 455 (2007) 157–168.
[44] L.W. Runnels, L. Yue, D.E. Clapham, The TRPM7 channel is inactivated by PIP2 hydrolysis, Nat. Cell Biol. 4 (2002) 329–336.
[45] Y. Yudin, V. Lukacs, C. Cao, T. Rohacs, Decrease in phosphatidylinositol 4,5-bisphosphate levels mediates desensitization of the cold sensor TRPM8 channels, J. Physiol. 15 (2011) 6007–6027.
[46] S. Brauchi, G. Orta, C. Mascayano, M. Salazar, N. Raddatz, H. Urbina, E. Rosenmann, F. Gonzalez-Nilo, R. Latorre, Dissection of the components for PIP2 activation and thermosensation in TRP channels, Proc. Natl. Acad. Sci. U. S. A. 104 (2007) 10246–10251.
[47] A. Rezvanpour, G.S. Shaw, Unique S100 target protein interactions, Gen. Physiol. Biophys. 28 (2009) F39–F46.
[48] X. Steinberg, C. Lespay-Rebolledo, S. Brauchi, A structural view of ligand-dependent activation in thermo TRP channels, Front. Physiol. 5 (2014) (eCollection2014).
[49] A.E. Lemmon, K.M. Ferguson, R. O'Brien, P.B. Sigler, J. Schlessinger, Specific and high-affinity binding of inositol phosphates to an isolated pleckstrin homology domain, Proc. Natl. Acad. Sci. U. S. A. 92 (1995) 10472–10476.
[50] B. Nilius, J. Prenen, G. Droogmans, T. Voets, R. Vennekens, M. Freichel, U. Wissenbach, V. Flockerzi, Voltage dependence of the Ca^{2+}-activated cation channel TRPM4, J. Biol. Chem. 278 (2003) 30813–30820.
[51] V. Lukacs, B. Thyagarajan, P. Varnai, A. Balla, T. Balla, T. Rohacs, Dual regulation of TRPV1 by phosphoinositides, J. Neurosci. 27 (2007) 7070–7080.
[52] A. Gericke, N.R. Leslie, M. Losche, A.H. Ross, PI(4,5)P2-mediated cell signaling: emerging principles and PTEN as a paradigm for regulatory mechanism, Adv. Exp. Med. Biol. 991 (2013) 85–104.
[53] S.B. Hansen, X. Tao, R. MacKinnon, Structural basis of PIP2 activation of the classical inward rectifier K^+ channel Kir2.2, Nature 477 (2011) 495–498.
[54] M.R. Whorton, R. MacKinnon, Crystal structure of the mammalian GIRK2 K^+ channel and gating regulation by G proteins, PIP2, and sodium, Cell 147 (2011) 199–208.
[55] Y. Kwon, T. Hofmann, C. Montell, Integration of phosphoinositide- and calmodulin-mediated regulation of TRPC6, Mol. Cell 23 (2007) 491–503.
[56] A. Penna, V. Juvin, J. Chemin, V. Compan, M. Monet, F.A. Rassendren, PI3-kinase promotes TRPV2 activity independently of channel translocation to the plasma membrane, Cell Calcium 36 (2006) 495–507.
[57] K. Prochazkova, R. Osicka, I. Linhartova, P. Halada, M. Sulc, P. Sebo, The *Neisseria meningitidis* outer membrane lipoprotein FrpD binds the RTX protein FrpC, J. Biol. Chem. 280 (2005) 3251–3258.
[58] L. Whitmore, B.A. Wallace, Protein secondary structure analyses from circular dichroism spectroscopy: methods and reference databases, Biopolymers 89 (2008) 392–400.
[59] Y. Zhang, I-TASSER server for protein 3D structure prediction, BMC Bioinforma. 9 (2008) 1–8.
[60] A. Roy, A. Kucukural, Y. Zhang, I-TASSER: a unified platform for automated protein structure and function prediction, Nat. Protoc. 5 (2010) 725–738.
[61] Molecular Operating Environment (MOE), Chemical Computing Group Inc., 1010 Sherbooke St. West, Suite #910, Montreal, QC, Canada, H3A 2R7, 2013.
[62] E.F. Pettersen, T.D. Goddard, C.C. Huang, G.S. Couch, D.M. Greenblatt, E.C. Meng, T.E. Ferrin, UCSF Chimera—a visualization system for exploratory research and analysis, J. Comput. Chem. 25 (2004) 1605–1612.
[63] B. Filippi, G. Borin, V. Moretto, F. Marchiori, Conformational properties of the N-terminal residues of S-peptide. II. The guanidine hydrochloride–water–trifluoroethanol system, Biopolymers 17 (1978) 2545–2559.
[64] J.W. Nelson, N.R. Kallenbach, Stabilization of the ribonuclease S peptide α helix by trifluoroethanol, Proteins Struct. Funct. Genet. 1 (1986) 211–217.
[65] S.I. Segawa, N. Fukuno, K. Fujiwara, Y. Noda, Local structures in unfolded lysozyme and correlation with secondary structures in the native conformation: helix-forming or -breaking propensity of peptide segment, Biopolymers 31 (1991) 497–509.
[66] M.A. Zaydman, J. Cui, PIP2 regulation of KCNQ channels: biophysical and molecular mechanisms for lipid modulation of voltage-dependent gating, Front. Physiol. 5 (2014) (e).
[67] K. Bodhinathan, P.A. Slesinger, Alcohol modulation of G-protein-gated inwardly rectifying potassium channels: from binding to therapeutics, Front. Physiol. 5 (2014) eCollection 2014.
[68] B.R. Pattnaik, S. Tokarz, M.P. Asuma, T. Schroeder, A. Sharma, J.C. Mitchell, A.O. Edwards, D.A. Pillers, Snowflake vitreoretinal degeneration (SVD) mutation R162W provides new insights into Kir7.1 ion channel structure and function, PLoS ONE 8 (2013) e71744.
[69] G. Khelashvili, G. Galli, H. Weinstein, Phosphatidylinositol 4,5-biphosphate (PIP2) lipids regulate the phosphorylation of syntaxin N-terminus by modulating both its position and local structure, Biochemistry 51 (2012) 7685–7698.
[70] K.A. Morales, T.I. Igumenova, Synergistic effect of $Pb2^+$ and PIP2 on C2 domain-membrane interactions, Biochemistry 51 (2012) 3349–3360.
[71] B.C. Suh, B. Hille, Regulation of ion channels by phosphatidylinositol 4,5-bisphosphate, Curr. Opin. Neurobiol. 15 (2005) 370–378.
[72] S. Ximena, C. Lespay-Rebolledo, S. Brauchi, A structural view of ligand-dependent activation in thermo TRP channels, Front. Physiol. 5 (2014) 1–14.
[73] J. Xie, B. Sun, J. Du, W. Yang, H.C. Chen, L. Yue, Phosphatidylinositol 4,5-bisphosphate (PIP(2)) controls magnesium gatekeeper TRPM6 activity, Sci. Rep. 1 (2011) (Epub).